RSC Advances




ROYAL SOCIETY OF CHEMISTRY

www.rsc.org/advances

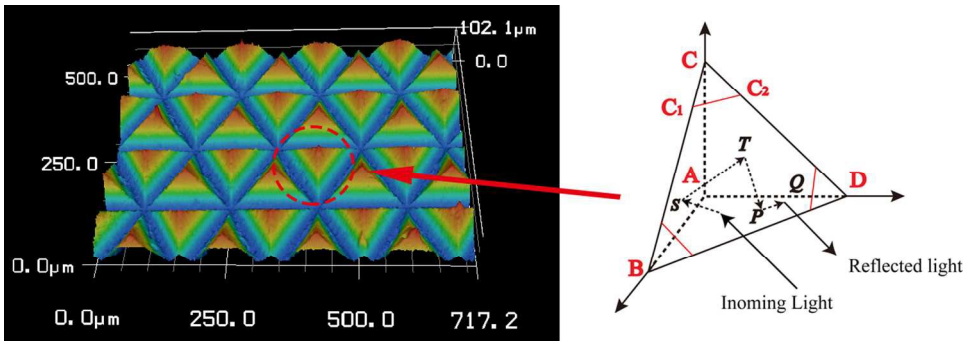


354x118mm (96 x 96 DPI)

Journal Name

ARTICLE

# Characterization of Polypropylene/Hydrogenated Styrene-Isoprene-Styrene Block Copolymer Blends and Fabrication of Micro-pyramids via Micro Hot Embossing of Blend Thin-films

Received 00th January 20xx,
Accepted 00th January 20xx

DOI: 10.1039/x0xx00000x

www.rsc.org/

Guiyang Jiang,[a] Chunwei Wang,[a] Zijin Liu,[a] Yinghao Zhai,[a] Yong Zhang*,[a]
Jie Jiang,[b] Nobuhiro Moriguchi,[b] Jun Zhu,[b] Yoshihiro Yamana[b]

Polypropylene (PP)/hydrogenated styrene-isoprene-styrene block copolymer (HYBRAR) blends were proposed as a new material for the fabrication of micro-pyramids via the micro hot embossing of their blend thin-films. As a typical thermoplastic amorphous polymer, HYBRAR could promote the crystallinity and decrease the crystallization temperature of PP. With increasing HYBRAR proportion, mechanical behavior of PP/HYBRAR blends changed from a typical plastic to a typical elastomer. HYBRAR exhibited higher complex viscosity and much higher storage modulus dependence on shearing frequency than PP, which is attributed to the strong interaction between polystyrene segments on HYBRAR. Measurement of micro-pyramids by a laser scanning microscope indicated the embossing temperature and HYBRAR proportion in the blends were the two key factors determining the integrity of micro-pyramids. With higher deformation ability than PP, HYBRAR could effectively promote the moldability of PP/HYBRAR blends in the micro hot embossing, leading to a better integrity of micro-pyramids and the low haze and high light transmittance of embossed thin-films. In addition, the effects of $T_m$ of PP and the thickness of the film base on the optical properties of embossed PP/HYBRAR blend thin-films were also discussed. PP/HYBRAR blends are proved to possess a promising prospect in the fabrication of optical thin-films.

## 1. Introduction

Micro hot embossing, a rapidly developing hot embossing duplicating technology in micro/nano scale,[1, 2] has be successfully applied in the fabrication of special microstructure patterns on the surface of thermoplastic polymers.[3] Enjoying the development of numerous new techniques, microstructure patterns have become central to a variety of applications, such as light collecting and antireflecting by microlens array (MLA),[3] bio and chemical micro electro mechanical system based micro-devices,[4] encoded information carrying by 3D microparticles,[5] discovery of novel drugs by DNA microarralys and dry adhesion by mushroom-shaped microfibers.[6, 7] According to the configuration of the molding tools, the micro hot embossing widely used in the fabrication of thin-films with special microstructure can be divided into three different kinds: plate-to-plate (P2P), roll-to-plate (R2P) and roll-to-roll (R2R). On the other hand, a favorable substrate material with good formability is the very basis for the fabrication of optical film via the hot embossing. Owing to the low cost, light weight, low molding temperatures and excellent optical properties, some thermoplastic polymers, such as poly(ethylene terephthalate),[8] polycarbonate,[9] poly(methyl methacrylate)[10, 11] and poly(vinyl chloride),[12, 13] have been successfully applied in the micro hot embossing. With adequate studies on the crystallization behavior,[14] optical properties,[15, 16] miscibility[17] and morphology,[18] polypropylene (PP) is also considered to have a promising potential application in the fabrication of optical films via micro hot embossing. As we know, higher degree of regularity of PP molecules results in a higher $T_m$ of PP, which is not good for its micro hot embossing. With the presence of small amount of ethylene segments, toughness of PP copolymer is higher than that of PP homopolymer. Apart from this, $T_m$ of PP is also expected to be much lower in the presence of ethylene segments. These two advantages endow PP copolymer with a higher deformation ability in the micro hot embossing. But due to the comparatively high $T_m$ of PP, blending modification by another elastomer with higher deformation ability is usually necessary.

A typical elastomer used in modified PP blends is HYBRAR, a new kind of styrene-isoprene-styrene block copolymer firstly produced by Kuraray Co., Ltd. Since firstly put into industrial production,

[a] School of Chemistry and Chemical Engineering, State Key Laboratory for Metal Matrix Composite Materials, Shanghai Jiao Tong University, Shanghai 200240, People's Republic of China.
E-mail: yong_zhang@sjtu.edu.cn
[b] Elastomer Department, Kuraray Co., Ltd., Tokyo 100-8115, Japan.

†Electronic Supplementary Information (ESI) available: [S1: The R2R micro hot embossing machine, S2: the measurement of the height of micro-pyramids]. See DOI: 10.1039/x0xx00000x

HYBRAR has already drawn much attention due to its successful applications in medical bags and tubing, sporting goods, automotive products and constructions. According to whether the rubber segments are hydrogenated or not, HYBRAR can be divided into non-hydrogenated and hydrogenated grades, molecular structure of the latter one is shown in Figure 1. Similar structure in PP and hydrogenated vinyl-polyisoprene segments of HYBRAR brings an important intermolecular interaction to them, which may partially improve the compatibility between PP and HYBRAR. And the heat and weather resistance of hydrogenated HYBRAR are much better than the non-hydrogenated one. So PP/HYBRAR blends in this work were prepared from PP and hydrogenated HYBRAR rather than non-hydrogenated one. Similar to styrene-butadiene-styrene triblock copolymer (SBS),[19] HYBRAR has polystyrene segments that act as physical crosslinking points and hydrogenated vinyl-polyisoprene segments in the rubbery state (Figure 1). It gives rise to a weak three-dimensional network and a microphase separation to HYBRAR, which have an important influence on the all performances of HYBRAR and its blends. Due to a very low crystallization ability resulting from the complex segments, the clarity of HYBRAR is much higher than that of PP. So the optical properties of PP/HYBRAR blends are much better than that of PP.

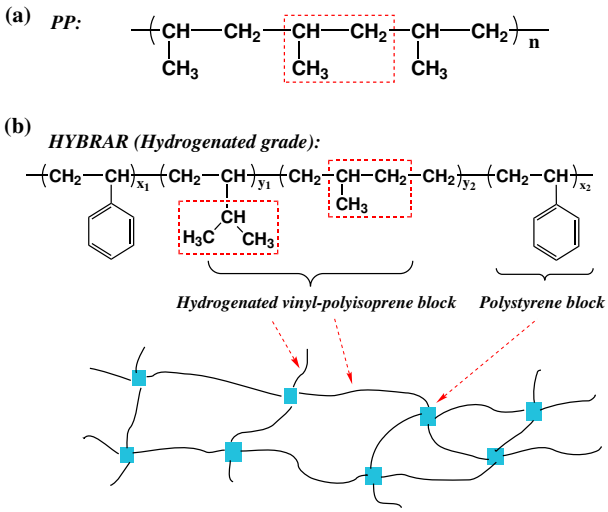


**Fig. 1** Structures of HYBRAR molecules (non-hydrogenated and hydrogenated grade) and the schematic diagram of its different blocks

And enjoying the very small crystallinity and low glass transition temperature ($T_g$), HYBRAR is expected to improve the moldability of PP in the micro hot embossing, which will greatly promote the application of PP/HYBRAR blends in the fabrication of optical thin-films. To the best of our knowledge, HYBRAR or PP/HYBRAR blends have not been reported used in the fabrication of optical thin-films via the micro hot embossing. In this work, PP/HYBRAR blends with different HYBRAR proportions were prepared and their crystallization behavior, mechanical properties and rheological behavior were studied. In the second part of this work, embossed thin-films with regular micro-pyramids on their surfaces were successfully fabricated from different PP/HYBRAR blends via a R2R micro hot embossing machine (Figure S1).[12] To evaluate the R2R process, laser scanning microscope was used to measure the height of micro-pyramids on the surface of embossed thin-films. And optical properties of embossed thin-films were also measured to evaluate the potential application of PP/HYBRAR blends in the fabrication of optical thin-films.

## 2. Experimental

### 2.1 Materials and fabrication

Hydrogenated HYBRAR (H7311, MFR: 5.7) with 12 wt% polystyrene segments was provided by Kuraray Co., Ltd, Japan. PP copolymer (GM1600E, MFR: 19) with 4.3 mol% ethylene segments was produced by Sinopec, China. PP/HYBRAR blends with HYBRAR proportion from 30% to 70% were made by a twin-screw extruder (ZE 25A, Berstorff, Germany). Theses blends along with PP and HYBRAR were compressed into sheets and thin-films with a thickness of 1 and 0.2 mm under 190 °C and 10 MPa on a hydraulic presses (LP-S-50, Labtech Engineering Co., Ltd, Thailand).

A roll-to-roll hot embossing system (Joint developed by Shanghai Jiao Tong University and Shanghai Forward Machinery Co., Ltd, China) with a specially designed thin metal mold was used to fabricate micro-pyramids on the surface of PP/HYBRAR thin-films. The depth of micro-pyramids shaped like pits on the metal mold was 72.6 μm. The fabrication was conducted under a constant roll speed of 0.1 m/min and at five different embossing temperatures: 110 °C, 120 °C, 130 °C, 140 °C and 150 °C.

### 2.2 Methods of characterization

Crystallization behavior of PP/HYBRAR blends was measured by DSC (Q 2000, TA Instruments, USA) at 10 °C/min using a $N_2$ flow. Heat flow curves were recorded after the thermal history having been eliminated. X-ray diffraction analysis was carried out with an X-ray diffractometer (D8 Advance, Bruker, Germany) from 5° to 80° at a scanning rate of 6° 2$\vartheta$/min.

Mechanical properties were measured at a rate of 50 mm/min on a material tester (Instron 4465, Instron Corp, USA) according to ASTM D638. And the hardness was determined using a Shore D durometer according to ASTM D2240. Thickness of above compressed sheets and embossed thin-films were measured by a thickness meter (2046S, Mitutoyo, Japan).

Rheological behavior of PP/HYBRAR blends was studied by a rotational rheometer (Gemini 200HR, Bohlin Instruments, UK). To determine the linear viscoelastic range, strain sweeps in the range of 0.01-100% at a frequency of 1 rad/s were carried out under 200

°C. And the frequency dependence of modulus and viscosity in the range of $10^{-2}$-$10^{2}$ rad/s at a strain of 1% were also studied under 200 °C. To study the effect of temperature on the rheological behavior, frequency sweep of the blends with 70% HYBRAR were also conducted at 170 °C.

The structure of micro-pyramids on the surface of embossed thin-films was measured by a laser scanning microscope (VK-210, Keyence Corporation, Japan) using the surface profile testing mode. And different magnifications of the objectives lens were adopted to measure different amounts of micro-pyramids.

The haze of PP/HYBRAR blend sheets and embossed thin-films was measured by a spectrophotometer (Color-Eye 7000A, X-rite, USA). The transmittance of embossed thin-films was measured by a special haze meter (M57, Diffusion System Co., Ltd, UK).

## 3. Results and Discussion

### 3.1. Crystallization behaviour

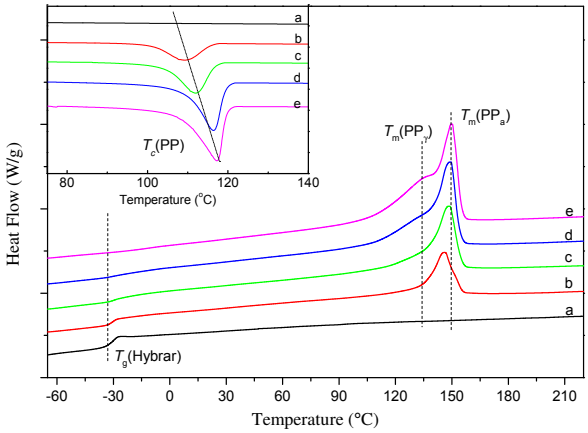


**Fig. 2** DSC melting and cooling curves of PP/HYBRAR blends with various HYBRAR proportions: (a) 100%; (b) 70%; (c) 50%; (d) 30%; (e) 0%.

The melting and cooling curves of PP/HYBRAR with different HYBRAR blends got from DSC experiments are depicted in Figure 2. In the investigated temperature range, a single $T_g$ for HYBRAR and a melting peak for PP are observed in the melting curves: about -30 °C and 147 °C, respectively. The movement ability of hydrogenated polyisoprene segments is higher than that of polystyrene segments. $T_g$ of polyisoprene is about -70°C, and it will not change too much after hydrogenation. $T_g$ of PS is about 100 °C, which is much higher than that of HYBRAR. So $T_g$ of HYBRAR is mainly related to the movement of hydrogenated polyisoprene segments. On the anther hand, PP used in our work is copolymer rather than homopolymer. In the presence of ethylene segments with higher movement ability, $T_m$ of PP is also lower than that of PP homopolymer.

$$X_C = \frac{\Delta H_m}{x \cdot \Delta H_{m-pp}} \times 100\% \quad (1)$$

Table 1 presents that with decreasing HYBRAR proportion decreasing from 100% to 0, the melting enthalpy ($\Delta H_m$) of samples increases from 0 to 70.5 J/g gradually. This big increment of $\Delta H_m$ mainly results from the decrement of HYBRAR proportion in blends. Crystallinity ($X_c$) of PP was calculated according to the Equation 1, in which $\Delta H_m$ is the melting heat, $x$ is the proportion of PP in blends and $\Delta H_{m\text{-}pp}$ is the melting heat for 100% crystalline PP, value of which used here is 165 J/g.[20] Table 1 shows that all $X_c$ of PP in PP/HYBRAR blends are about 45%, which are obviously higher than that of neat PP. And due to the presence of ethylene segments (4.3 mol%) in PP copolymer, $X_c$ of all samples are all lower that 50%. On the other hand, Table 1 shows that with increasing HYBRAR from 0 to 70%, the crystallization temperature ($T_c$) of PP decreases from 117.6 to 109.3 °C gradually. In contrast to this, $T_c$ of PP and other polymers are usually known to increase with the addition of the nucleating agent. And the amount of HYBRAR is much higher than that of a nucleating agent. So it can

**Table 1.** Crystallization Parameters of PP/HYBRAR Blends Measured by DSC and XRD

| Crystallization Parameters | HYBRAR Proportion: | | | | |
|---|---|---|---|---|---|
| | 100% | 70% | 50% | 30% | 0% |
| $T_g$/°C | -29.7 | -29.8 | -29.7 | -30.1 | -- |
| $T_m$/°C | -- | 145.8 | 148.2 | 149.0 | 149.6 |
| $\Delta H_m$/(J/g) | -- | 22.3 | 37.0 | 53.1 | 70.5 |
| $T_c$/°C | -- | 109.3 | 112.1 | 116.4 | 117.3 |
| $\Delta H_c$/(J/g) | -- | 24.8 | 42.5 | 56.9 | 69.3 |
| $X_c$ (DSC)/% | 0 | 45.1 | 44.8 | 46.0 | 42.4 |
| $H_{040}/H_{130}$ | -- | 1.787 | 2.246 | 3.076 | 3.909 |
| $H_{300}/H_{130}$ | -- | 0.726 | 0.734 | 0.870 | 1.093 |
| $X_c$ (XRD)/% | 0 | 46.4 | 43.4 | 49.6 | 45.0 |

be concluded that though the crystallinity of PP/HYBRAR blends is higher than that of neat PP, HYBRAR is not a nucleating agent for PP. The decrease in $T_c$ of PP found here is related to two important reasons. The first one is that with the addition of HYBRAR, PP can be seen in a concentrated HYBRAR solution and therefore the nucleation process of PP is restrained.[21] The second one is that the viscous HYBRAR and the strong molecular interactions between PP and HYBRAR can slow the diffusion of PP chains during the crystallization process.[22] So with higher HYBRAR proportions, PP/HYBRAR blends tends to crystallize at lower temperature. A smaller shoulder in front of the melting peak in neat PP and PP/HYBRAR blends with 30% HYBRAR is observed. This should be ascribed to the melting process of *β*-form or *γ*-form PP crystals that is less stable than *α*-form PP.[21] With increasing HYBRAR proportion, the shoulder becomes less obvious and the exothermic peak becomes much narrower. And similar tendency is also observed in the cooling curves. This phenomenon clearly indicates the suppression effect of HYBRAR on β-form or γ-form PP crystals is much larger than that on the α-form PP crystals.

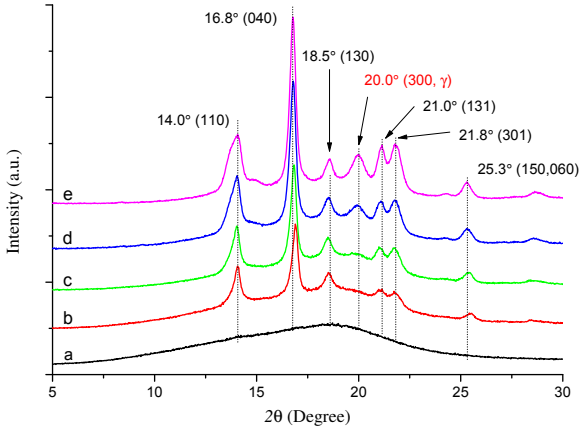


**Fig. 3** X-ray diffraction patterns of PP/HYBRAR blends with various HYBRAR proportions: (a) 100%; (b) 70%; (c) 50%; (d) 30%; (e) 0%.

According to the XRD patterns shown in Figure 3, there is no any diffraction peak on the XRD pattern belonging to neat HYBRAR, which indicates the crystallinity of HYBRAR is very low. This also proves HYBRAR's lacking of any impurities for the crystallization of PP. For neat PP and PP/HYBRAR blends, there are six obvious diffraction peaks appearing at 2$\vartheta$ of 14.0°, 16.8°, 18.5°, 21.0°, 21.8° and 25.3°, which correspond to the (110), (040), (130), (131), (301) and (110+060) planes respectively.[20, 23-26] This proves the crystallization of PP phase is mainly *α*-form crystal and the proportion of (040) plane is the biggest one among all planes. The height ratio of (040) and (130) planes increasing from 1.787 to 3.909 (Table 1) indicates that the effect of HYBRAR on the (040) plane is also much more obvious than that on other planes. The β-form crystal is not observed in this type of PP, whose diffraction at 2$\vartheta$ of 16.5° corresponds to the (300) plane.[24] In addition, a diffraction peak corresponding to the (300) plane of *γ*-form crystal is also observed at 2$\vartheta$ of 20.0°.[27] The type of PP and the cooling process mainly contribute to the formation of this crystal of PP. Similar to the results of DSC experiments, the diffraction peak of *γ*-form crystal becomes not obvious when HYBRAR is higher than 50%. With increasing HYBRAR proportion, the height ratio of peaks at 300 and 130 planes decreases from 1.093 to 0.726 (Table 1). With increasing HYBRAR from 0 to 100%, intensities of all these diffraction peaks decrease obviously while the height of amorphous region baseline increases gradually. The $X_c$ of PP/HYBRAR blends calculated from XRD is similar to that calculated from DSC. This indicates the proportion of the amorphous region in the blends increases while the crystalline phase region decreases gradually due to the increase of HYBRAR proportion.

### 3.2 Mechanical properties

Figure 4 shows the stress-strain curves of PP/HYBRAR blends with different HYBRAR proportions. With increasing HYBRAR proportion from 0 to 100%, the stress-strain curve of blends changes from a typical elastomer to a typical plastic. Due to the physical crosslinking of polystyrene segments, the stress-strain curve of neat HYBRAR is very close to that of a common rubber. And when the HYBRAR proportion is 30% and 0, a yielding stress occurs during the stretching process and the yield strength of these two blends is 12.2 and 31.7 MPa, respectively. This indicates with a low HYBRAR proportion, PP/HYBRAR blends can maintain a plastic-like tensile behavior. With the HYBRAR increasing from 30 to 70%, the tensile strength (*TS*) decreases from 25.2 MPa to 12.2 MPa and the elongation at break (*EB*) increases from 793% to 905%. But for neat PP, the *EB* is much lower and *TS* is smaller than that of blends with 30% HYBRAR. This is because HYBRAR is a typical elastomer with high *EB* and low *TS* while PP is a typical plastic with low *EB* and high *TS*. On the other hand, the hardness increases from 9 to 72 when PP proportion increases from 0 to 100%, which also should be ascribed to the crystallization of PP.

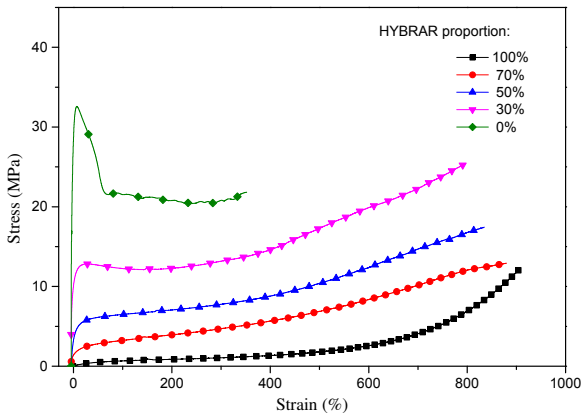

**Fig. 4** Strain-stress curves of PP/HYBRAR blends with different HYBRAR proportions

### 3.3. Rheological Behavior

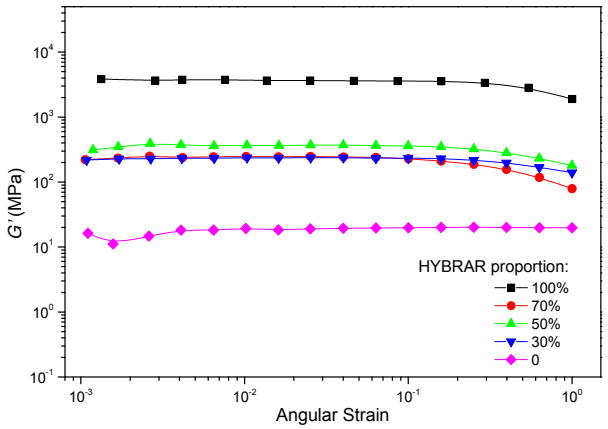


**Fig. 5** Strain dependence of *G'* for PP/HYBRAR blends with different HYBRAR proportions

Figures 5 and 6 show the results of strain and frequency sweeps in rheological experiments. In Figure 5, the storage modulus (*G'*) of neat HYBRAR is much higher than that of neat PP and PP/HYBRAR blends with different HYBRAR proportion. This should be ascribed to the strong interaction between polystyrene segments of HYBRAR and the higher molecular weight of HYBRAR. In addition, when the HYBRAR proportion is 0, 30, 50, 70 and 100%, the linear viscoelastic region range of PP/HYBRAR blends is 0.4%~100%, 0.07%~25.0%, 0.12%~15.9%, 0.11%~10.0% and 0.07%~16.0%, respectively. This indicates that increasing HYBRAR proportion can sharply shorten the linear viscoelastic region of PP/HYBRAR blends.

Figure 6 shows the effect of HYBRAR proportion on the frequency dependence of *G'*, loss modulus (*G''*) and complex viscosity ($\eta^*$). It can be clearly seen that the dynamic modulus and viscosity of these five samples show completely different dependences on the sweep frequency. On the one hand, due to the stronger interaction between HYBRAR molecules, both of *G'* and *G''* increase gradually with increasing HYBRAR from 0 to 100%. On the other hand, *G'* and *G''* of all samples both increase gradually with increasing investigated frequency from $10^{-2}$ to $10^{2}$ Hz, which indicates these two components and their blends are all pseudoplastic fluid.[28] In the presence of PP, terminal zone respectively appears on *G'* and *G''* curves at the low frequency range.[20] For neat PP, the slope of *G'* and *G''* curves in this terminal zones are 1.9 and 1, respectively, indicating

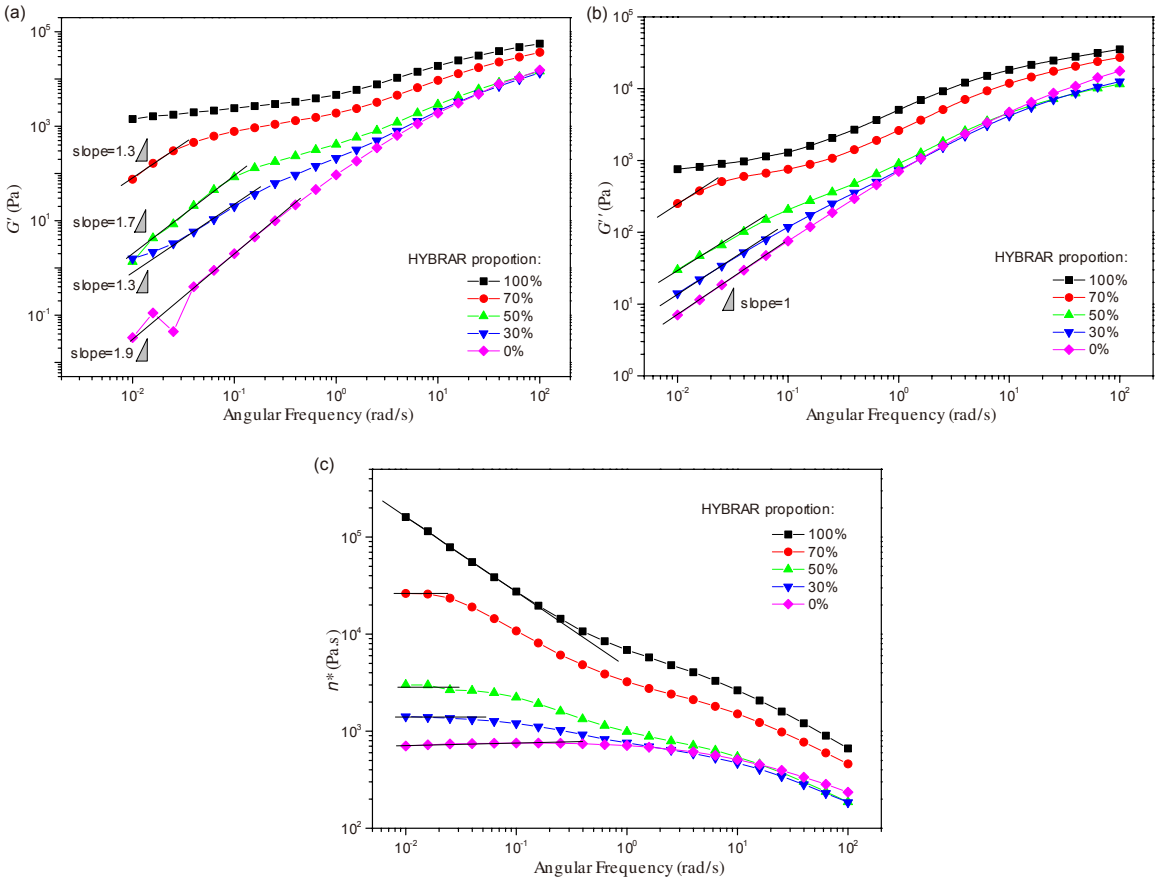

**Fig 6**. Frequency dependence of (a) $G'$, (b) $G''$ and (c) $\eta^*$ for PP/HYBRAR blends with various HYBRAR proportions

that PP has an obvious liquid-like terminal behavior as $G' \propto \omega^{1.9}$ and $G'' \propto \omega$.[29] But for neat HYBRAR, there is a pseudo-plateau in $G'$ and $G''$ curves at the low frequency range. This should be ascribed to the existence of a weak three-dimensional network of HYBRAR, which results from the polystyrene segments that can act as the crosslinking points. With increasing HYBRAR proportion, both the frequency range and slope of $G'$ curves in the terminal zones decrease gradually (Figure 6a). When the HYBRAR proportion are 30, 50 and 70%, the slopes of $G'$ at the terminal zone are 1.3, 1.7 and 1.3 respectively while all slopes of $G''$ for different blends are 1 (Figure 6b). This change in the slope of $G'$ indicates the behavior of PP/HYBRAR blends at low frequency range shifts from liquid-like to solid-like gradually with increase of HYBRAR proportion. And it can also be concluded that the frequency dependence of PP/HYBRAR blends decreases significantly with increasing HYBRAR proportion from 0% to 100%.

Figure 6c shows that with increasing HYBRAR proportion from 0% to 100%, the $\eta^*$ of PP/HYBRAR blends increases gradually, which confirms that the intermolecular interaction of HYBRAR is higher than that of PP. It is also observed that $\eta^*$ at the low frequency range of HYBRAR is much higher than PP and PP/HYBRAR blends, where the rheological behavior depends on the size of the molecular chain coil and the interaction between molecules. This increment of elasticity and relaxation time proves a phase-separated morphology at low frequency range.[28, 30] According to the above analysis, this phenomenon is also related to the interaction between polystyrene segments in HYBRAR molecules. With increasing frequency, $\eta^*$ of HYBRAR decreases sharply while there is a pseudo-plateau in $\eta^*$ curves of neat PP and PP/HYBRAR blends. This should be ascribed to that the interaction between HYBRAR molecules is easily damaged when the frequency increases. But the interaction between PP molecules is so insensitive to the frequency that it will not change obviously until the frequency reaches a very high value (Figure 6c). As a result, a platform persists in a very long frequency range. According to the frequency dependence of blends with 70% HYBRAR at low frequency range (Figure 7a), PP/HYBRAR blends are liquid-like at 200 °C as $G'<G''$ and $G' \propto \omega^{1.3}$, $G'' \propto \omega^{0.8}$ while they are solid-like at 170 °C as $G'>G''$ and $G' \propto \omega^{0.4}$, $G'' \propto \omega^{0.2}$. And the pseudo-plateau in $\eta^*$ curve (Figure 7b) disappears when the temperature decreases from 200 to 170 °C. This is related to the order-disorder transition of HYBRAR at this temperature range. When temperature is 170 °C, polystyrene segments of HYBRAR are still under order state. With the presence of the supermolecular structure of HYBRAR that results from the strong interaction between polystyrene segments, frequency dependence of $\eta^*$ at low frequency range is still obvious. But when temperature increases to 200 °C, which is higher than the order-disorder transition temperature of HYBRAR, polystyrene segments are in disorder state. And most of the supermolecular structure disappears with the disappearance of the strong interaction between polystyrene segments. As a result, the frequency dependence of $\eta^*$ at low frequency range becomes very small. This indicates rheological properties of HYBRAR and its blends above the order-disorder transition temperature are very similar to those of molten homopolymer. It can be concluded that excepting the temperature, proportion of HYBRAR and the interaction between polystyrene segments are the two crucial factors determining the rheological behavior of PP/HYBRAR blends.

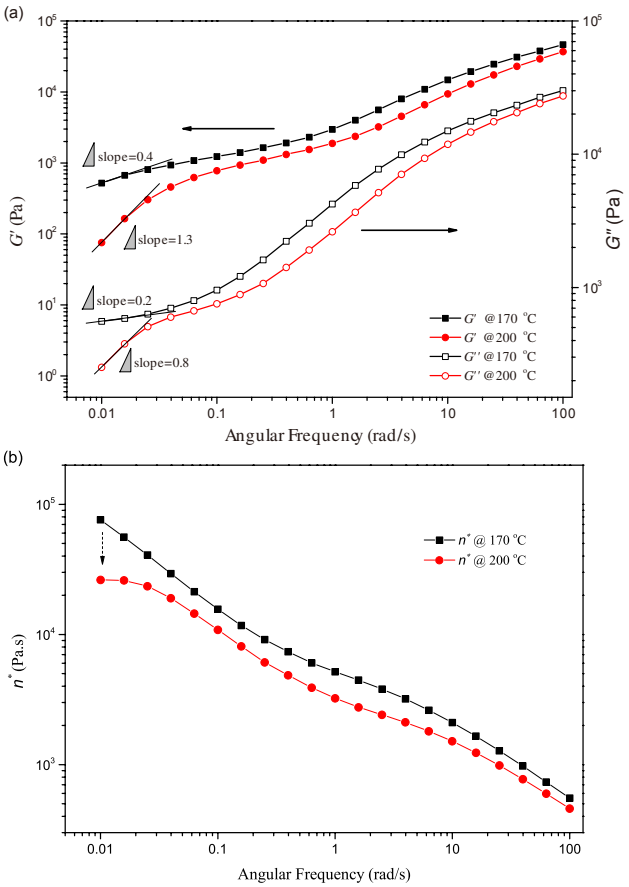


**Fig 7.** Frequency dependence of (a) $G'$, $G''$ and (b) $\eta^*$ for PP/HYBRAR blends with 70% HYBRAR 170 °C and 200 °C

### 3.4. Microstructure of thin-films surface

Due to the very high deformability, neat HYBRAR is difficult to be made into thin-films. To compare the formability of other PP/HYBRAR blends, the microstructure on the surface of thin-films fabricated from other PP/HYBRAR blends were measured by a laser microscope, and results are shown in Figure 8. The regular arrangement of the micro-pyramids with different heights and the

morphology of single micro-pyramid can be clearly observed. With increasing embossing temperature from 110 to 130 °C, the micro-pyramids on the thin-films with 70% HYBRAR become much fuller and the heights of them became much bigger (Figure 8a and e). But

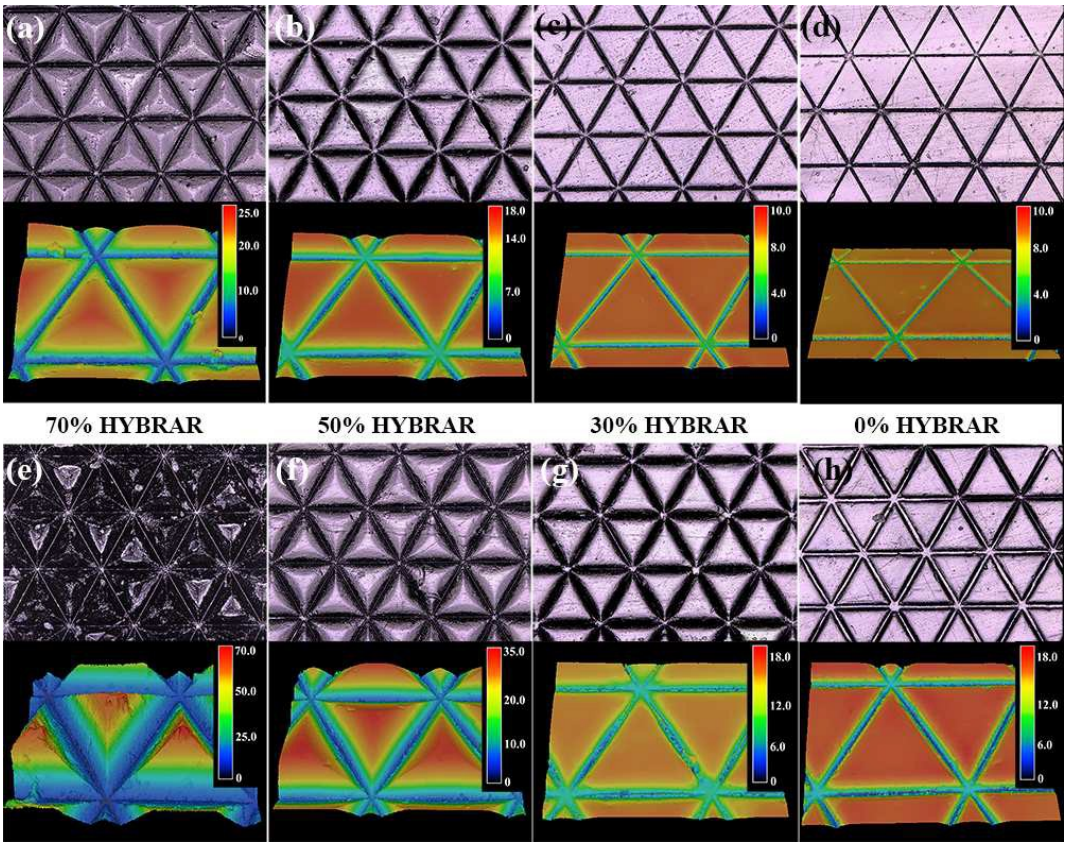


**Fig 8.** Laser microscope images of micro-pyramids on the embossed thin-films with different HYBRAR proportions and fabricated at two temperatures: (a) ~ (d): 70~0% HYBRAR at 110 °C; (e) ~ (h): 70~0% HYBRAR at 130 °C. (The unit of scale bar is μm)

with the same increment of temperature, height of the micro-pyramid on neat PP thin-film was almost the same (Figure 8d and h).

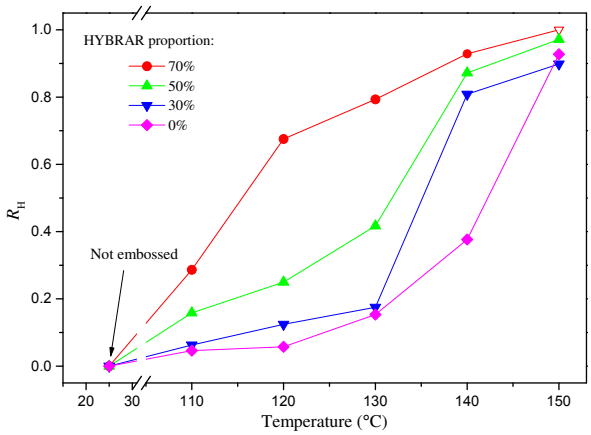


**Fig 9.** Height ratio ($R_H$) of micro-pyramids on embossed thin-films with different HYBRAR proportions and fabricated at different embossing temperatures.

Different parameters were chosen to evaluate the R2R hot embossing process. Deng[12] used the average height of three random micro-pyramids and the proportion of those micro-pyramids with a critical height. Yun[31] used the patterning ratio of the depth of the mold and that of the pattern on the embossed thin-film. And Yeo[32] chosen the averaged depth of 10 embossed micro-channels. In this work, the height of micro-pyramids is related to the optical properties of embossed thin-films. To implement a quantitative evaluation of the micro hot embossing formability of PP/HYBRAR blend, we chose the height ratio ($R_H$) of the height of micro-pyramids ($H_i$) and the depth of pits on the R2R embossing mold ($H_0$). The standard for the measurement of $H_i$ and $H_0$ is shown in Figure S2. Figure 9 shows $R_H$ of the thin-films prepared from four different PP/HYBRAR blends and embossed at different embossing temperatures. And $R_H$ of thin-films without embossing are seen as that of thin-films embossed at 25 °C, value of which are all 0. On the one hand, with increasing embossing temperature from 110 to 150 °C, $R_H$ of embossed thin-film increases from 0 to 1 gradually. This is highly attributed to the improvement of moldability of all PP/HYBRAR blends with increasing embossing

temperature from 110 to 150 °C. When the embossing temperature increases from 140 to 150 °C, $R_H$ of neat PP increases from 0.376 to 0.927 sharply. This is related to the significant improvement of moldability when the embossing temperature is higher than the $T_m$ of PP. For other PP/HYBRAR blends, the same change occurs at a lower temperature. This temperature is defined as the necessary embossing temperature ($T_n$), and its values for these four samples are 120, 140, 140 and 150 °C. It can be concluded the necessary embossing temperature for crystalline polymers like PP may be higher than their $T_m$ and the addition of an amorphous polymer like HYBRAR can reduce the effect of the crystallization on the necessary embossing temperature.

On the other hand, $R_H$ of thin-films embossed at the same temperature increases gradually with increasing HYBRAR proportion from 0 to 70%, which may be ascribed to the higher deformation ability of HYBRAR and the decrease of the whole crystallinity of thin-films. Especially, when the embossing temperature is 120 °C, $R_H$ of PP/HYBRAR (30/70) blend is over than 0.7 while that of PP is only 0.05. This difference forcefully proves the significant enhancement of HYBRAR on the formability of PP in the micro embossing. But when the temperature is up to 150 °C, micro-pyramids cannot be fabricated on the thin-film with 70% HYBRAR. At this temperature, the thin-film is very soft and the interfacial adhesion between the micro-pyramids and the mold is excessively strong. As a result, many micro-pyramids will be damaged when stripped from the mold and the thin-film cannot be kept intact. In other word, when the embossing temperature is 150 °C the $R_H$ of thin-film with 70% HYBRAR is up to maximum and it can be seen as 1.

### 3.5 Optical properties of embossed thin-film

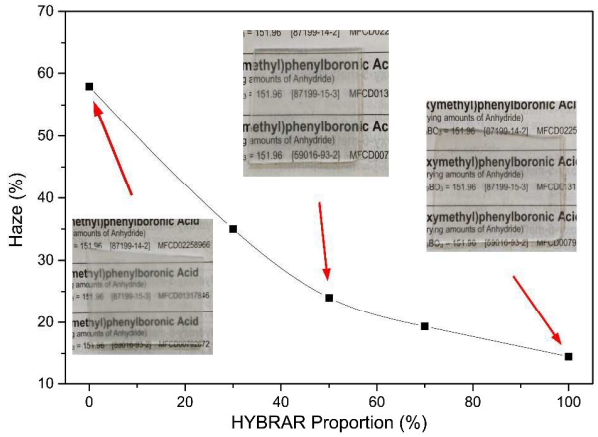


**Fig. 10** Haze of sheets made by PP/HYBRAR blends with different HYBRAR proportions

Haze and clarity, which can reflect the turbidity and sharpness of optical materials respectively, are often used to study the optical properties of polymers blends and their thin-films.[15, 33, 34] In this work, values of haze and transmittance are measured to characterize the optical properties of PP/HYBRAR blends. For different PP/HYBRAR blends, haze of compressed sheets with a thickness of 2 mm is shown in Figure 10. With increasing HYBRAR proportion from 0% to 100%, the haze of PP/HYBRAR blends gradually decreases from 58 to 15, indicating the turbidity of PP/HYBRAR blends decreases markedly. Though the crystallinity of PP component in PP/HYBRAR blends is higher than that of neat PP and the size of PP spherulites can be affected by the addition of HYBRAR,[34] the change in optical properties should be mainly ascribed to the increase of HYBRAR proportion.

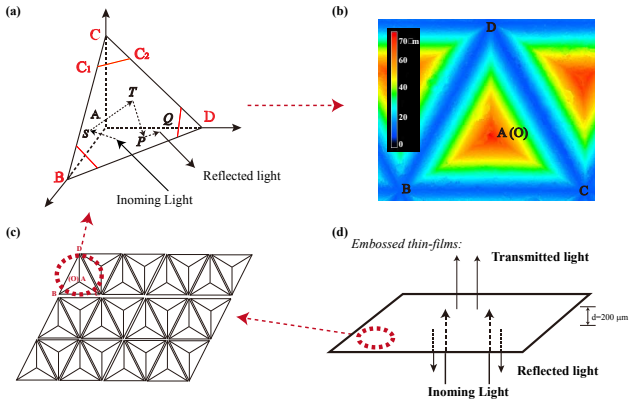


**Fig 11.** The optical principle and structure of micro-pyramids: (a) total reflect through single micro-pyramid, (b) laser microscope image of single micro-pyramid, (c) arrangement of micro-pyramids on the surface of embossed thin-films and (d) schematic diagram of integral optical path

As shown in Figure 11c, micro-pyramids on the surfaces of these embossed thin-films can be seen as a kind of MLA. In this study, the optical properties of embossed thin-films were measured with the light entering the MLA from the bottom of micro-pyramids. According to the study of Lin[13], if the light enters from the bottom of the pyramids, it can be divided into three major parts: direct recycle, effective refraction and indirect recycle. As shown in Figure 11a, if the micro-pyramid on the embossed thin-films is in full shape, its three side faces are very smooth and perpendicular to each other. Analysis of optical path by vector method proves that the emitting light from the bottom of the micro-pyramids will go back from the bottom of micro-pyramids after three total reflections on the three side faces. And the directions of incoming and reflected light are parallel to each other. This reflected light is the indirect recycle part and it is the largest one of the three major parts under optimal condition. But when the light enters in the micro-pyramids from the area marked as $\Delta CC_1C_2$ in Figure 11a, this direct recycle will not happen. The area where the direct recycle can happen is called as the effective area of direct recycle or direct reflection and its value is 66.7% when the micro-pyramid is in full shape. On the other hand, due to the limit of the critical angle

necessary for the total reflection, the light will be refracted out of the film from the front of the film or reflected first and then refracted out. Light of these two parts along with the light that does not enters via the effective area will be measured as the transmitted light (effective refraction). Similar to the transmitted light, the indirect recycle is also thought to take up smaller proportion on the optimal condition (Figure 11d). According to this theoretical model, the height of the micro-pyramids and the defects of the side faces are two key factors determining the final haze and transmittance of embossed thin-films. With the $R_H$ of micro-pyramids increasing and the defects on the side faces reducing, the proportion of reflected light increases and that of the transmitted light decreases. As a result, the haze of the embossed thin-film will increase while the transmittance decreases.

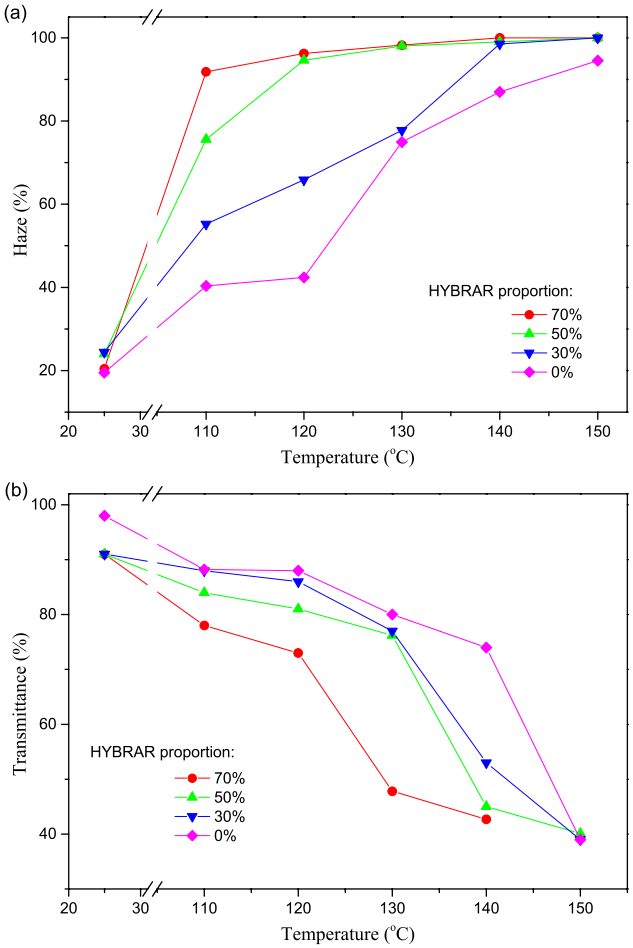


Fig. 12 (a) Haze and (b) transmittance of embossed thin-films with different HYBRAR proportions and fabricated at different embossing temperatures

According to the haze and transmittance of thin-films embossed at different temperatures (Figure 12), with increasing embossing temperature from 110 to 150 °C, the haze of embossed thin-films increases gradually while the transmittance decreases a lot. Apart from this, for the thin-films embossed at the same temperature, the haze increases and the transmittance decreases with increasing HYBRAR proportion from 0 to 70%. This is related to the big increase in the integrity of micro-pyramids when the embossing temperature is higher than $T_m$ of PP. These two change trends forcefully illustrate the effects of embossing temperature and composition of blends on the optical properties of embossed thin-films. And this also indirectly reflects the temperature and composition dependences of the micro-embossing formability. It is noteworthy that the transmittance decrease rapidly when the embossed temperature reaches $T_n$. And because haze is the flux ratio of the scatted light with a critical scattering angle (±2.5°) and the incoming light, so the haze values of all PP/HYBRAR blends are already close to 100% and the effect of embossing temperature become not obvious when the embossing temperature reaches 140 °C or higher. But when the haze is close to 100%, the transmittance is much higher than 0, which proves the angle of the left transmitted light is smaller than ±2.5°. To sum up, the embossing temperature undoubtedly contributes a lot to the optical properties of embossed thin-films by affecting the integrity of micro-pyramids the embossed thin-films.

As shown in Figure 12, haze and transmittance of thin-films not embossed are seen as that of thin-films embossed at 25 °C. Noteworthy is that compared to those sheets with the thickness of 1 mm (Figure 10), the haze of these thin-films decrease greatly to near 20%. And at this thickness, the difference between values of the haze and transmittance for thin-films with different HYBRAR proportions no longer exists. With the thickness of thermoplastic polymers increasing, their haze usually increases while the transmittance decreases gradually, which is ascribed to the effect of material size.[10] And according to the results of the simulation, there will be a big difference between the theoretical model and the experimental data when the thickness of base under the micro-pyramids reaches a certain value. So it can be speculated that the thickness of the base under micro-pyramids also has an important effect on the optical properties of embossed thin-films.

## Conclusions

PP/HYBRAR blends with different HYBRAR proportions were prepared and their thin-films with micro-pyramids on the surface were successfully fabricated via the micro hot embossing. As the diffusion of PP chains were suppressed by the strong molecular interactions during the crystallization, a decrease in the $T_c$ of PP was observed. With increasing HYBRAR proportion, storage modulus and elasticity of PP/HYBRAR blends both increased gradually. Physical crosslinking in HYBRAR with high shearing frequency and temperature dependences accounted for this. Regular micro-pyramids on the surface severed as a kind of microlens array and most of light entering from its bottom went back or was consumed.

With the addition of HYBRAR, the integrity of micro-pyramids and the optical properties of embossed PP/HYBRAR blend thin-films both significantly improved a lot, which should be mainly attributed to the higher deformation of HYBRAR.

## Acknowledgements

Financial support from the National Natural Science Foundation of China (Grant No. 51235008, 51273109) is gratefully acknowledged.

## References

1. M. Worgull, M. Schneider, M. Röhrig, T. Meier, M. Heilig, A. Kolew, K. Feit, H. Hölscher and J. Leuthold, RSC Advances, 2013, 3, 20060.
2. B. Wu and T. Özel, in Micro-Manufacturing, John Wiley & Sons, Inc., 2011, DOI: 10.1002/9781118010570.ch6, pp. 159-195.
3. C. Jiang, X. Li, H. Tian, C. Wang, J. Shao, Y. Ding and L. Wang, ACS Appl. Mater. Interfaces, 2014, 6, 18450-18456.
4. R. K. Jena, K. Dev, C. Y. Yue and A. Asundi, RSC Advances, 2012, 2, 5717.
5. H. C. Jeon, S. G. Han, S.-G. Park and S.-M. Yang, RSC Advances, 2012, 2, 2334.
6. M. Geissler, E. Roy, G. A. Diaz-Quijada, J. C. Galas and T. Veres, ACS Appl. Mater. Interfaces, 2009, 1, 1387-1395.
7. W. Bin Khaled and D. Sameoto, ACS Appl. Mater. Interfaces, 2014, 6, 6806-6815.
8. S. J. Liu and Y. C. Huang, Opt. Express, 2009, 17, 18083-18092.
9. J. T. Wu, S. Y. Yang, W. C. Deng and W. Y. Chang, Microelectron. Eng., 2010, 87, 1951-1954.
10. 10 L. Peng, Y. Deng, P. Yi and X. Lai, J. Micromech. Microeng., 2014, 24, 013001.
11. 11 P. Schneider, C. Steitz, K. H. Schafer and C. Ziegler, Phys. Status Solidi A, 2009, 206, 501-507.
12. Y. Deng, P. Yi, L. Peng, X. Lai and Z. Lin, J. Micromech. Microeng., 2014, 24, 045023.
13. L. W. Lin, T. K. Shia and C. J. Chiu, J. Micromech. Microeng., 2000, 10, 395-400.
14. Y. Pang, X. Dong, X. Zhang, K. Liu, E. Chen, C. C. Han and D. Wang, Polymer, 2008, 49, 2568-2577.
15. M. J. Abad, A. Ares, L. Barral, J. Cano, F. J. Diez, S. Garcia-Garabal, J. Lopez and C. Ramirez, J. Appl. Polym. Sci., 2004, 94, 1763-1770.
16. A. Menyhárd, M. Gahleitner, J. Varga, K. Bernreitner, P. Jääskeläinen, H. Øysæd and B. Pukánszky, Eur. Polym. J., 2009, 45, 3138-3148.
17. C. Álvarez, A. Martínez-Gómez, E. Pérez, M. U. de la Orden and J. Martínez Urreaga, Polymer, 2007, 48, 3137-3147.
18. S. Sinha Ray, S. Pouliot, M. Bousmina and L. A. Utracki, Polymer, 2004, 45, 8403-8413.
19. B. X. Fu, A. Lee and T. S. Haddad, Macromolecules, 2004, 37, 5211-5218.
20. M. El Achaby, F.-E. Arrakhiz, S. Vaudreuil, A. el Kacem Qaiss, M. Bousmina and O. Fassi-Fehri, Polym. Compos., 2012, 33, 733-744.
21. J.-H. Chen, J.-C. Zhong, Y.-H. Cai, W.-B. Su and Y.-B. Yang, Polymer, 2007, 48, 2946-2957.
22. L. Li, L. Chen, P. Bruin and M. A. Winnik, J. Polym. Sci., Part B: Polym. Phys., 1997, 35, 979-991.
23. A. R. Bhattacharyya, T. V. Sreekumar, T. Liu, S. Kumar, L. M. Ericson, R. H. Hauge and R. E. Smalley, Polymer, 2003, 44, 2373-2377.
24. L. Wang and J. Sheng, Polymer, 2005, 46, 6243-6249.
25. C. Saujanya and S. Radhakrishnan, Polymer, 2001, 42, 6723-6731.
26. B. X. Yang, J. H. Shi, K. P. Pramoda and S. H. Goh, Composites Sci. Technol., 2008, 68, 2490-2497.
27. H. Xia, Q. Wang, K. Li and G.-H. Hu, J. Appl. Polym. Sci., 2004, 93, 378-386.
28. Y. Di, S. Iannace and L. Nicolais, J. Appl. Polym. Sci., 2002, 86, 3430-3439.
29. S. Liu, W. Yu and C. Zhou, Polymer, 2014, 55, 2113-2124.
30. H. S. Jeon, A. I. Nakatani and C. C. Han, Macromolecules, 2000, 33, 9732-9739.
31. D. Yun, Y. Son, J. Kyung, H. Park, C. Park, S. Lee and B. Kim, Rev. Sci. Instrum., 2012, 83, 015108.
32. L. P. Yeo, S. H. Ng, Z. Wang, Z. Wang and N. F. de Rooij, Microelectron. Eng., 2009, 86, 933-936.
33. P. M. Kristiansen, A. Gress, P. Smith, D. Hanft and H.-W. Schmidt, Polymer, 2006, 47, 249-253.
34. M. Kristiansen, M. Werner, T. Tervoort and P. Smith, Macromolecules, 2003, 36, 5150-5156.



 